

## Full-length Article

## Sex differences in the effects of PARP inhibition on microglial phenotypes following neonatal stroke

Christiane Charriaut-Marlangue<sup>a</sup>, Claire Leconte<sup>b</sup>, Zsolt Csaba<sup>a</sup>, Linda Chafa<sup>a</sup>, Julien Pansiot<sup>a</sup>, Mustapha Talatizi<sup>a</sup>, Kristin Simon<sup>b</sup>, Raffaella Moretti<sup>a</sup>, Catherine Marchand-Leroux<sup>b</sup>, Olivier Baud<sup>a,c</sup>, Valérie C Besson<sup>a,b,\*</sup>

<sup>a</sup> U1141 PROTECT, INSERM, Université Paris Diderot, Sorbonne Paris Cité, Hôpital Robert Debré, 48 boulevard Sérurier, 75019 Paris, France

<sup>b</sup> EA4475 – Pharmacologie de la Circulation Cérébrale, Faculté de Pharmacie de Paris, Université Paris Descartes, Sorbonne Paris Cité, 4 avenue de l'Observatoire, 75006 Paris, France

<sup>c</sup> Division of Neonatology and Pediatric Intensive Care, Children's University Hospital of Geneva and University of Geneva, Geneva, Switzerland

## ARTICLE INFO

## Keywords:

Amygdala  
Cortex  
Microglial phenotype  
Neonatal stroke  
Neurobehavioral deficits  
Poly (ADP-ribose) polymerase inhibitor

## ABSTRACT

Neonatal acute ischemic stroke is a cause of neonatal brain injury that occurs more frequently in males, resulting in associated neurobehavioral disorders. The bases for these sex differences are poorly understood but might include the number, morphology and activation of microglia in the developing brain when subjected to stroke. Interestingly, poly (ADP-ribose) polymerase (PARP) inhibition preferentially protects males against neonatal ischemia. This study aims to examine the effects of PJ34, a PARP inhibitor, on microglial phenotypes at 3 and 8 days and on neurobehavioral disorders in adulthood for both male and female P9 mice subjected to permanent middle cerebral artery occlusion (pMCAo). PJ34 significantly reduced the lesion size by 78% and reduced the density of CX3CR1<sup>gfp</sup>-labeled microglial cells by 46% when examined 3 days after pMCAo in male but not in female mice. Eight days after pMCAo, the number of Iba1<sup>+</sup>/Cox-2<sup>+</sup> cells did not differ between male and female mice in the cortical peri-infarct region. In the amygdala, Iba1<sup>+</sup>/Cox-2<sup>+</sup> (M1-like) cell numbers were significantly decreased in PJ34-treated males but not in females. Conversely, Iba1<sup>+</sup>/Arg-1<sup>+</sup> (M2-like) and Arg-1<sup>+</sup>/Cox-2<sup>+</sup> (Mtransitional) cell numbers were significantly increased in PJ34-treated females. Regarding neurobehavioral disorders during adulthood, pMCAo induced a motor coordination deficit and a spatial learning deficit in female mice only. PJ34 prevented MBP fibers, motor coordination and learning disorders during adulthood in female mice. Our data show significant sex differences in the effects of PARP inhibition on microglia phenotypes following neonatal ischemia, associated with improved behavior and myelination during adulthood in females only. Our findings suggest that modulating microglial phenotypes may play key roles in behavior disorders and white matter injury following neonatal stroke.

## 1. Introduction

Neonatal arterial stroke is a cerebrovascular event that occurs near the time of birth, characterized by pathological or radiological evidence of focal arterial infarction primarily affecting the middle cerebral arterial territory, with an incidence of 1/2800 to 1/5000 live births (Nelson, 2007). Neonatal stroke produces significant morbidity and severe long-term neurological and cognitive deficits, including cerebral palsy, epilepsy, neurodevelopmental disabilities, impaired vision and language function, and emotional symptoms (Sigurdardottir et al., 2010; Coq et al., 2016). Currently, there is no specific treatment for neonatal stroke. The current strategy is primarily focused on supportive

care, including the management of neonatal seizures. Male sex is recognized to be a risk factor for cerebral palsy during the perinatal period, and ischemic injury appears to be more common in boys, regardless of lesion type (Golomb, 2009; Golomb et al., 2004).

The number, morphology and activation of microglial cells differ during brain development depending on the gender (Nissen, 2017; Charriaut-Marlangue et al., 2018), suggesting that microglial cells might react differently towards stroke in females than in males. According to the environment and the production of cytokines, microglia can adopt an inflammatory/cytotoxic phenotype (M1-like) and/or an immunomodulatory/repairing phenotype (M2-like) (Hu et al., 2017), although the question of whether and how these changes occur can vary

\* Corresponding author at: EA4475 – Pharmacologie de la Circulation Cérébrale, Faculté de Pharmacie de Paris, Université Paris Descartes, Sorbonne Paris Cité, 4 avenue de l'Observatoire, 75006 Paris, France.

E-mail address: [valerie.besson@parisdescartes.fr](mailto:valerie.besson@parisdescartes.fr) (V.C. Besson).

<https://doi.org/10.1016/j.bbi.2018.05.022>

Received 27 November 2017; Received in revised form 25 May 2018; Accepted 27 May 2018  
Available online 28 May 2018

0889-1591/ © 2018 Elsevier Inc. All rights reserved.

according to species (zebrafish vs rodent), models (*in vitro* vs *in vivo*), and brain developmental stages (immature vs mature) (Ransohoff, 2016). According to its environment and production of cytokines microglia can adopt an inflammatory/cytotoxic phenotype (M1-like) and/or immunomodulatory/repairing phenotype (M2-like) (Hu et al., 2017), although this polarizing question is raised according to species (zebrafish vs rodent), models (*in vitro* vs *in vivo*), and brain developmental stages (immature vs mature) (Ransohoff, 2016). Microglia/macrophage activation and polarization remains under debate, and it is now proposed to evaluate microglia polarization according to a stimulus- and disease-specific understanding based on transcriptomic and proteomic profiling (Jassam et al., 2017). During brain injury, microglia cells were traditionally considered to be purely toxic. However, data show that microglia can play both injurious (Monje et al., 2003; Iosif et al., 2006) and beneficial (Faustino et al., 2011) roles after ischemia. Age-dependent microglial activation has been investigated during hypoxia-ischemia in the immature (postnatal days 9 and 30, P9 and P30) brain. Interestingly, injured brains at P9 show a dramatic increase in microglial activation and a predominant pro-inflammatory response soon after hypoxia-ischemia compared to brain injury at P30, suggesting that the inhibition of microglial activation might be beneficial in the immature brain (Ferrazzano et al., 2013).

Poly (ADP-ribose) polymerases (PARPs) are a large family of constitutive nuclear enzymes (Endres et al., 1997) that are involved in transcriptional regulation, cell division and cell death (Besson, 2009; Berger et al., 2018). Indeed, PARP has been demonstrated to promote the expression of pro-inflammatory genes, which contribute to the pathology of many diseases (Curtin and Szabo, 2013). PARP1 interacts with a number of transcription factors and co-factors, including NF- $\kappa$ B, NFAT, AP-1, YY1, SP1, and SIRT1, which have been associated with inflammatory gene expression (Bai and Virág, 2012). Moreover, PARP inhibition (Ducrocq et al., 2000; Joly et al., 2003) and PARP gene disruption preferentially reduce infarct lesions in males, in a neonatal hypoxic-ischemic model (Hagberg et al., 2004), and after ischemia, in young adult mice (Liu et al., 2011), and differentially modulates microglial phenotypes in adult males and females (review in Chen et al., 2014).

The aim of this study is to examine, in males and females, the effect of PARP inhibition on microglial phenotypes (3 and 8 days after ischemia) and on neurobehavioral disorders and myelination (2 to 3 months after ischemia) in P9 mice subjected to ischemia after permanent middle cerebral artery occlusion (pMCAo, Moretti et al., 2016). We focused on the peri-lesional cortex and the amygdala because it has been recently reported that altered amygdala development might be linked to alterations in white matter connectivity (Cismaru et al., 2016), leading to behavior alterations in babies. It has also been observed that the amygdala displays anatomic and functional gender discrepancies (Im et al., 2018). Moreover, we evaluated white matter injury (WMI) because (1) it is one of the consequences of brain injury in babies that have suffered from neonatal arterial stroke, and (2) it is the underlying cause of motor and cognitive disabilities in these children (Back, 2017).

## 2. Materials and methods

### 2.1. Ethics statement

All care and experiments were performed with ethical approvals from the Robert Debré Hospital Research Council Review (license A75-19-01, 08/28/2013), in accordance with French regulations and the European Union Council Directive of September 22, 2010 (2010/63/EU) on the protection of animals for experimental use.

### 2.2. Animals

C57BL6/J mice (WT) were purchased from Janvier Labs (Le Genest-

St Isle, France.  $n = 32$ ). CX3CR1<sup>gfp</sup>/CCR2<sup>rfp</sup> transgenic mice, which have the green fluorescent protein gene knocked into one allele of CX3CR1 (CX3CR1<sup>gfp</sup>) and the red fluorescent protein gene knocked into one allele of C-C motif Chemokine receptor-2 (CCR2<sup>rfp</sup>) (Saederup et al., 2010), were provided by Dr. C. Combadiere (INSERM U1135, 75013 Paris, France) ( $n = 73$ ). Males and females were both used and housed under a standard 12 h light:dark cycle. The total number of animals used in this study was 126 mice (25 litters). Three animals (2 treated with 0.9% NaCl and 1 with PJ34) died during the first 24 h after pMCAo.

For behavior, mice were housed in fixed unisex groups (5–6 mice/cage) after weaning for the length of the experiment, as housing conditions affect behavior (Prendergast et al., 2014). As a control, 19 non-operated naive mice (9 M and 10 F) were evaluated.

### 2.3. Ischemia

Permanent proximal middle cerebral artery (MCA) occlusion (pMCAo) was performed in P9 male and female C57BL/6J mice under isoflurane anesthesia in 30% O<sub>2</sub> and 70% N<sub>2</sub>O. Mice were sacrificed at 3 days (CX3CR1<sup>gfp</sup>/CCR2<sup>rfp</sup> mice;  $n = 32$ ; 15 M and 17 F), 8 days (WT C57BL6/J mice;  $n = 34$ ; 18 M and 16 F), and 3 months after pMCAo (CX3CR1<sup>gfp</sup>/CCR2<sup>rfp</sup> mice; stroke  $n = 41$ ; 21 M and 20 F; non-operated  $n = 19$ ; 9 M and 10 F). There were no differences in the weight at P9 (before ischemia) between the different groups of animals (see Supplemental Table 1).

Investigators who performed neurobehavioral tests, infarct volume measurements, tissue loss and Myelin Basic Protein (MBP) density measurements, and cell counting were blinded to the group assignments.

According to our previous reported studies,  $n = 6$  animals were sufficient for immunohistochemistry (Moretti et al., 2016). Previous estimated effect size was calculated using the BiostaTGV software (<https://marne.u707.jussieu.fr/biostatgv>) with an alpha risk of 0.05.

### 2.4. Drug treatment

Three sets of experiments were designed (see Supplementary Fig. 1 for an outline of the experimental procedures, number and strain of mice used, and data measured).

In the first set of experiments, animals were randomly divided into 2 groups and treated with either 0.9% NaCl or PJ34 (10 mg/kg, Sigma-Aldrich, France), given intraperitoneally (i.p.) 1 day after pMCAo.

In the second and third sets of experiments, animals were randomly divided into 2 groups and treated with either 0.9% NaCl or PJ34 (10 mg/kg, i.p.) 1 and 3 days after pMCAo.

### 2.5. Cell death and immunohistochemistry

Coronal 16- $\mu$ m thick cryostat sections (CX3CR1<sup>gfp</sup>/CCR2<sup>rfp</sup> mice 3 days after ischemia) were stained with the TUNEL assay (nuclear staining), using the “In situ Cell Death Detection” Kit (AbCys, Paris, France) according to manufacturer instructions.

Coronal 16- $\mu$ m thick paraffin sections (WT C57BL6/J mice) at the hippocampal level (corresponding to 4.83 mm in the “Atlas of the developing mouse brain at P6”) were stained using rabbit anti-Iba1 (RRID: AB\_839504; 1:1000), rabbit anti-Cox2 (RRID: AB\_2085144; 1:200), and goat anti-Arginase-1 (RRID: AB\_2227469; 1:200) antibodies. For immunofluorescence, secondary antibodies coupled with the green marker Fluorophore S488 (Interchim, Montluçon, France) or the red fluorescent marker cyanine 3 (Jackson Immuno-Research Laboratories, West grove, PA) were used.

For confocal imaging, sections (CX3CR1<sup>gfp</sup>/CCR2<sup>rfp</sup> mice 3 days after ischemia) were analyzed using a Leica TCS SP8 confocal scanning system (Leica Microsystems, Wetzlar, Germany) equipped with 405-nm Diode, 488-nm Argon, 561-nm DPSS and 633-nm HeNe lasers. Optical

sections were collected using the 20× HC PL APO CS2 objective (numerical aperture 0.75). For each optical section, quadruple-fluorescence images were acquired in sequential mode to avoid potential contamination by fluorescence emission cross-talk. The settings for laser intensity, beam expander, pinhole (1 Airy unit), range property of emission window, electronic zoom, gain and offset of photomultiplier, field format, and scanning speed were optimized initially and held constant throughout the study so that all sections were digitized under the same conditions. The tilescan acquisitions and the subsequent merging of mosaics were produced using the Leica LAS AF software (Leica Microsystems). Fluorescent cell populations were identified in the regions of interest and counted using the Cell Counter plugin of FIJI/ImageJ software (<http://fiji.sc/Fiji>). Images were equally adjusted for brightness and contrast, and composite illustrations were built in Adobe Photoshop CS3 (Adobe Systems, San Jose, CA).

## 2.6. Cell quantification

Iba-1, Arg-1 and Cox-2 positive cells were counted in a blind manner in the penumbra region of three coronal sections per animal at 3 and 8 days after ischemia using a 20× objective. Iba-1-Arg-1 and Iba-1-Cox-2 double-positive cells were counted in the same regions with a 40× lens, and then merged images were created with FIJI/ImageJ software.

## 2.7. MBP density

Coronal 16-μm thick cryostat sections (CX3CR1<sup>gfp</sup>/CCR2<sup>gfp</sup> mice 3 months after ischemia, at the level of the MCA territory) were stained using the mouse anti-MBP (RRID\_9497; 1:500) antibody. Quantification of MBP was done on 8-bit digital images collected using a high-resolution video camera (2560 × 1920 pixels) interfaced with a Nikon microscope under a 4× objective (numerical aperture 0.25). Illumination and camera settings were maintained at the same level for image acquisition for all images. For each experimental group, 3 sections were imaged from 6 animals. Immunoreactive signal was segmented and counted using the Fiji distribution (Schindelin et al., 2012) of ImageJ. Results were expressed as density of immunoreactivity in regions of interests containing all 6 layers of the cortex.

## 2.8. Behavioral experiments

Evaluations of sensorimotor performance and motor coordination (pole test), locomotor activity (actimetry), exploration and defense behavior (open field, elevated plus maze and marble burying tests) and cognitive performance (Barnes maze) were performed, according to previously published protocols (Taib et al., 2017), between 2 months (day 62) and 3 months (day 107) after pMCAo, which corresponds with the adult stage (see Supplementary Fig. 2 for an outline of the experimental and behavioral procedures).

Three groups of C57Bl6 CX3CR1<sup>gfp</sup>/CCR2<sup>gfp</sup> mice were used: non-operated (male: n = 9; female: n = 10), stroke + NaCl (male: n = 11; female: n = 10) and stroke + PJ34 (given at 1 and 3 days post-ischemia; male: n = 10; female: n = 8).

### 2.8.1. Actimetry

The horizontal (locomotion) and vertical (rearing) activities were individually assessed in transparent activity cages (20 × 10 × 12 cm), using automatic monitoring of photocell beam breaks (Imetronic, Bordeaux, France). The actimetry test was performed on day 62 (2 months), recording every 10 min for 1 h and then every 30 min for 22 h.

### 2.8.2. Elevated plus maze

Defense behavior was evaluated on days 71–72 after pMCAo, using the elevated plus maze, which relies on the animals' preference for dark

enclosed arms over bright open arms. This task assesses the willingness of the mouse to explore the open arms of the maze, which are fully exposed and at an elevated height. Time spent in the open arm decreases in mice that exhibit anxiety-like behavior. The maze consisted of a Plexiglas plus-shaped platform elevated 50 cm from the floor, with 4 arms intersecting at a 90° angle, creating 4 individual arms that were each 37 cm long and 6 cm wide. The 2 closed arms were shielded by 14 cm-high side and end walls, while the 2 open arms had no walls. The arms are connected to each other by a central platform (6 × 6 cm).

The mouse was placed on the central platform, facing one of the open arms. The mouse was allowed to explore the maze for a 9-min period (540 s), while the number of entries and the time spent in each of the arms were recorded by a videotrack system (Viewpoint) every 3 min. As advised by File (2001), data were presented as % time spent in the open arms = [(time spent in open arms entries)/(total time: 540 s) × 100].

### 2.8.3. Open-field

The open-field test, performed on day 73 after pMCAo, is commonly used to evaluate exploratory and defense behavior in rodents. The open-field test was performed using a square, white, open-field apparatus (40 × 40 × 45 cm), made of plastic permeable to infrared light. The distance traveled (evaluating locomotor activity), time spent in inactivity and in the center of the open-field, and the number of entries in the center (evaluating defense behavior), were recorded by a videotrack system (Viewpoint®) every 5 min during the 15 min test. A blinded investigator counted the number of rearings (evaluating exploration behavior).

### 2.8.4. Pole test

This test consists of a vertical round pole covered with a rough surface (50 cm in length, 8 mm in diameter) and has been used to reveal adult pMCAo-induced motor coordination deficits (Bouët et al., 2007). This test was performed from days 76 to 78 after pMCAo to evaluate the motor coordination learning. The mouse was placed at the top of the pole, head up. The ability of the mice to turn and descend from the top was assessed over five trials of 3 min maximum per day.

### 2.8.5. Marble-burying test

The obsessive-compulsive-like behavior was assessed with the marble-burying test. This test was performed on day 79 after pMCAo (Taylor et al., 2017). Each mouse was placed in a transparent activity cage (28 × 13 × 15 cm), lined with over 5 cm of litter. On the top of the litter, 18 marbles (1.5 cm diameter) were homogeneously placed, and the mouse was freely allowed to bury the marbles over a 30 min period. The number of marble buried was recorded each minute for the first 5 min and then every 5 min for the remaining 25 min.

### 2.8.6. Barnes maze test

This task is commonly used to evaluate spatial learning and memory performance in rodents, as it requires an escape response (Barnes, 1979; Sharma et al., 2010). The maze is a wet, white and circular platform (80 cm diameter), that is brightly illuminated (400 lx) and raised 50 cm above the floor, with 18 holes (5 cm) equally spaced around the perimeter. A white hidden escape box (8 × 5 × 5 cm), representing the target, was located under one of the holes.

Prior to the test, each mouse was subjected to a habituation trial where the mouse was directly placed into the escape box for 30 s.

**Learning:** the mouse was placed in the center of the circular maze and was allowed to explore the platform and holes for 3 min maximum. The distance traveled was recorded using a videotrack system (Viewpoint®). Latency to reach the escape box and the number of errors (number of empty holes visited) were manually noted. When the mouse found and entered the escape box, the videotrack recording was stopped, and the mouse remained in the escape box for 10 s before being returned to its home cage. If the mouse did not enter

spontaneously, it was gently placed into the escape box, before being returned to its home cage. On the first day of training, mice underwent 2 trials after the habituation trial; thereafter, 3 trials were performed per day, with a 2 h inter-trial interval.

**Probe trial:** on the 5th day of learning (or reversal learning), the probe trial, in which the escape box is removed and which lasts for 1 min, is used to assess spatial memory performance. The time spent and the distance traveled in each sextant (defined as one of the 6 sections of the maze, including 3 holes) were recorded. The target zone is defined as the section that contains the target hole and the two adjacent holes.

**Reversal learning:** mice underwent 3 trials per day, with a 2 h inter-trial interval, for four days to learn a new location of the escape box. On the fifth day, a probe trial was performed.

## 2.9. Statistics

Data are expressed as the mean  $\pm$  SEM of  $n$  observations.

All figures and statistical analyses were created with GraphPad Prism 5.0 (GraphPad Software, San Diego, CA). Lesion volume, cell counts, tissue loss, MBP density were analyzed using a one-way ANOVA, followed by the Newman-Keuls test. MBP density was analyzed using the non-parametric Kruskal-Wallis test followed by Dunn's Multiple Comparison Test. Data collected from the actimetry and pole tests were analyzed using a 2-way ANOVA for repeated measures, followed by a Dunnett test. Data collected from the open field, elevated plus maze, and marble burying tests were analyzed using a one-way ANOVA followed by the Dunnett test. Data from the learning and reversal learning trials of the Barnes maze were analyzed using a one-way ANOVA for area under a curve, and a two-way ANOVA for repeated measures was used for the distance traveled, followed by a Dunnett test. Data from the probe trials of the Barnes maze were analyzed using a two-way ANOVA for repeated measures, followed by a univariate Student's  $t$  test, to compare to the theoretical value of 16.67% (dotted line, i.e., when the mouse spent equal time within each sextant) for retention, and a Dunnett test for comparison between groups for the target sextant.  $p < 0.05$  was considered statistically significant.

## 3. Results

### 3.1. Effect of PJ34 on lesion, microglial activation and cell death 3 days after neonatal stroke

The mean cortical infarct volume at 3 days after pMCAo was not significant between males (M) and females (F) [M:  $9.5 \pm 5.7 \text{ mm}^3$  ( $n = 8$ ); F:  $10.6 \pm 11.0 \text{ mm}^3$  ( $n = 9$ )] in NaCl-treated mice. In contrast, PJ34, a PARP inhibitor, significantly reduced the lesion size in M [ $2.9 \pm 2.2 \text{ mm}^3$  ( $n = 7$ ),  $p < 0.05$ ] but not in F [ $15.8 \pm 9.7 \text{ mm}^3$  ( $n = 8$ )] mice (Fig. 1A and B). Cell death was observed with TUNEL<sup>+</sup> nuclei in the cortical lesion (Fig. 1C, enlarged panel) but not observed in remote regions (i.e., the amygdala, as shown in Supplemental Fig. 3).

CX3CR1<sup>gfp</sup>/CCR2<sup>gfp</sup> mice were used to assess the effect of PJ34 on microglial cells and macrophages (Fig. 1D–O). A large number of CX3CR1<sup>gfp</sup> labeled-microglial cells, with a round and amoeboid morphology, were detected in the peri-infarct region (including the sub-cortical white matter) in both M (Fig. 1D, E and M) and F (Fig. 2A and B) NaCl-treated mice. In PJ34-treated M mice, the density of CX3CR1<sup>gfp</sup>-labeled microglia significantly decreased when compared to NaCl-treated mice (Fig. 1O). CCR2<sup>gfp</sup>-labeled macrophages were sparsely detected in the lesion, for both M (Fig. 1G and K) and F (not shown) mice. CCR2<sup>gfp</sup>-labeled macrophages did not localize with CX3CR1<sup>gfp</sup>-labeled microglia (Fig. 1M). Cox-2 protein was observed in the peri-infarct, both in CX3CR1<sup>gfp</sup>-microglia and cortical cells (Fig. 1L). CCR2<sup>gfp</sup>-labeled macrophages did not express the Cox-2 protein (Fig. 1N). The density of CCR2<sup>gfp</sup>-macrophages and Cox-2<sup>+</sup> cells did not significantly differ between PJ34- and NaCl-treated mice (Fig. 1O).

We then observed a differential Arg-1 protein expression, which was close to the basal level in male mice. In contrast, a stronger protein expression was observed in female mice, for both NaCl- and PJ34-treated animals (Fig. 2A–D). Arg-1 protein expression did not co-localize with the CX3CR1<sup>gfp</sup>-labeled microglia. Arg-1-positive cells were scattered in the peri-infarct region (Fig. 2D) and were primarily present in the meninges as fusiform cells (white arrows in Fig. 2E).

### 3.2. Effect of PJ34 on tissue loss and microglial activation 8 days after neonatal stroke

Eight days after pMCAo, lesions significantly increased in volume and became cystic, as previously reported (Moretti et al., 2016). Two doses of PJ34 (given 1 and 3 days following ischemia) did not reduce the tissue loss in either M [NaCl:  $19.2 \pm 9.3\%$  ( $n = 9$ ); PJ34:  $16.0 \pm 12.0\%$  ( $n = 9$ )] or F [NaCl:  $15.4 \pm 7.7\%$  ( $n = 7$ ); PJ34:  $11.2 \pm 6.5\%$ , ( $n = 9$ )] mice (Fig. 3A).

The number of Iba-1<sup>+</sup> microglial cells (with both ramified and/or amoeboid morphology) did not differ between M and F mice or between NaCl- and PJ34-treated mice in the cortical peri-infarct region (Fig. 3B). The number of Cox-2<sup>+</sup> cells was similar among the four groups of animals (Fig. 3C), and most of the Cox-2 labeling co-localized with Iba-1<sup>+</sup> microglia/macrophages (Fig. 3D). No Arg-1<sup>+</sup> cells were observed in the cortical peri-infarct region.

Using cresyl violet-stained sections, we observed that degenerative cells (see Supplemental Fig. 4) were present in the amygdala (lateral and basolateral amygdaloid nucleus), and we therefore quantified microglia cells. Iba-1<sup>+</sup> ramified microglia cells were found at similar numbers among the four groups of animals (Fig. 4A). Iba-1<sup>+</sup> cells displayed small cell bodies with thin, long and highly branched processes. The number of Cox-2<sup>+</sup> cells and double-labeled Iba-1<sup>+</sup>/Cox-2<sup>+</sup> (M1-like) cells was significantly decreased in PJ34-treated M mice compared to NaCl-treated M mice ( $p < 0.05$ ), while no difference was observed between NaCl- and PJ34-treated F mice (Fig. 4B and D). The number of Arg-1<sup>+</sup> cells was not different among the four groups of animals (Fig. 4C); however, the number of double-labeled Iba-1<sup>+</sup>/Arg-1<sup>+</sup> (M2-like) cells significantly increased in PJ34-treated F mice ( $p < 0.05$ ) compared to NaCl-treated F mice (Fig. 4E and G). In addition, most Cox-2<sup>+</sup> cells also expressed Arg-1<sup>+</sup> protein (Mtrans, Fig. 4F), and their number significantly increased in PJ34-treated F mice compared to NaCl-treated F mice, whereas no difference was observed between NaCl- and PJ34-treated M mice (Fig. 4H).

### 3.3. Effect of PJ34 on behavior, tissue loss and myelination in adulthood after neonatal stroke

#### 3.3.1. Sensorimotor performances

During the actimetry test, spontaneous locomotor activity evolved over a 23-hour period, with a decrease during the first hour, corresponding to the habituation phase, and an increase just before the dark phase, corresponding to the active 12-hour period, as described in the literature (Dispersyn et al., 2017). There were no significant differences between groups, for either horizontal activity (Fig. 5A and B, for M and F mice, respectively) or rearings (data not shown), suggesting that the effects observed in the other behavioral tests are not related to changes in spontaneous locomotor activity.

The pole test did not reveal any deficit in any M group. M mice learned the motor coordination task, as the time to turn decreased with repeated training days (Fig. 5C, time effect  $p < 0.0001$ ). F mice exhibited a deficit in motor coordination learning (Fig. 5D, interaction  $p = 0.052$ , time effect  $p < 0.001$ ). NaCl stroke F mice had an increased time to turn compared to other female groups on the second day of training ( $p < 0.05$ ), suggesting that neonatal ischemia in F mice only impaired motor coordination learning, which was abolished by PJ34 treatment ( $p < 0.05$ ).

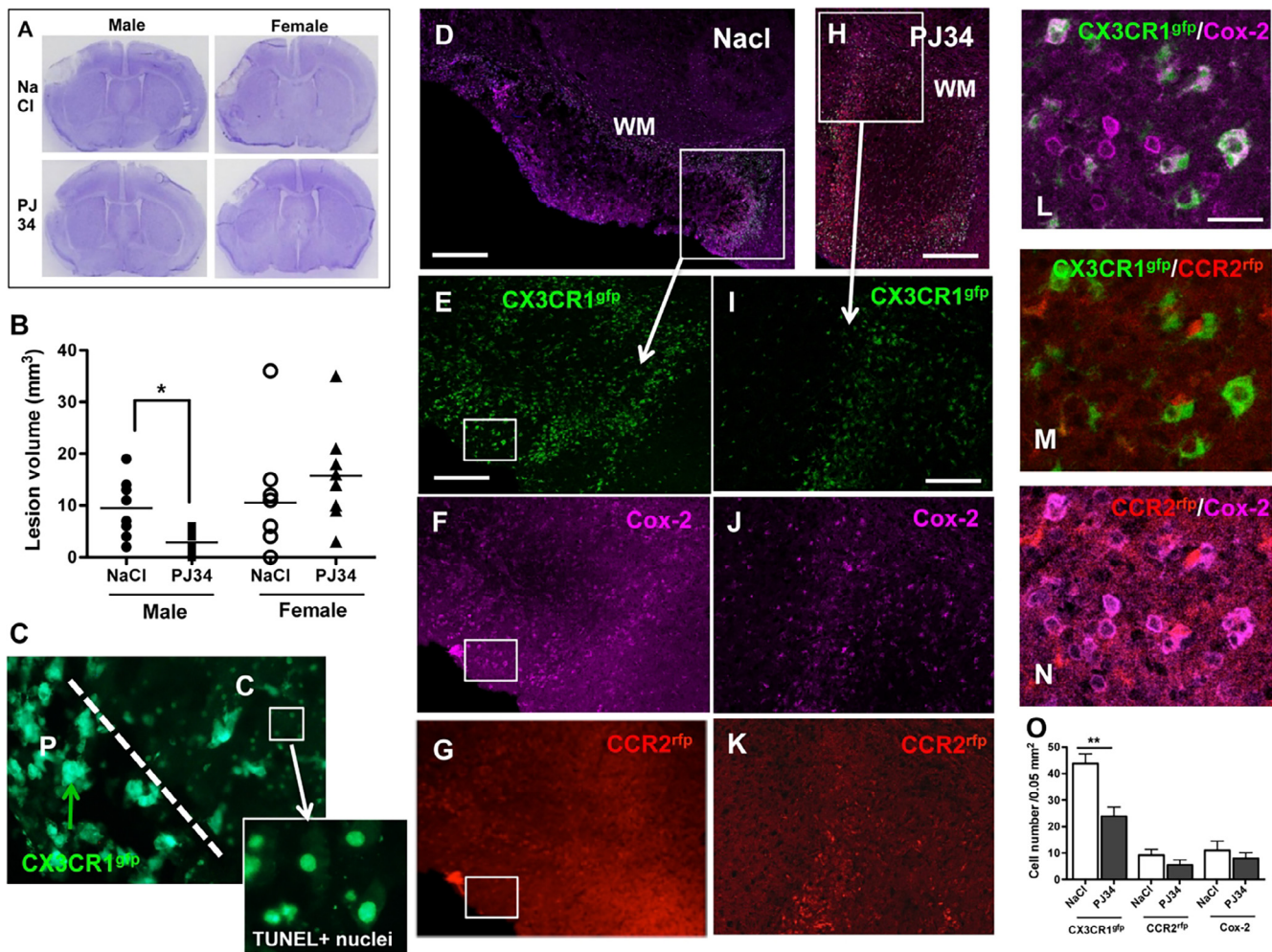


**Fig. 1.** Effect of PJ34 on lesion size and microglial activation 3 days after pMCAo in CX3CR1<sup>gfp</sup>/CCR2<sup>rfp</sup> mice (Male and Female: A and B; Male: C to N). PJ34 or NaCl was given 1 day after pMCAo by a single intraperitoneal injection. A-B: Cortical lesions in males and females at 3 days. C: TUNEL assay in a cortical section. Note the presence of CX3CR1<sup>gfp</sup> microglia in the peri-infarct region (P) and TUNEL<sup>+</sup> nuclei in the infarct region (C, core) in a NaCl-treated male. D-N: Confocal merged images of labeled cells in the peri-infarct region in NaCl- (D) and PJ34-treated mouse (H). E and I: Enlarged panels showing CX3CR1<sup>gfp</sup>-labeled microglia (green). F and J: Cox-2-labeled cells (magenta). G and K: CCR2<sup>rfp</sup>-labeled macrophages (red). L-N: Double labeling of CX3CR1<sup>gfp</sup> and Cox-2 (L), CX3CR1<sup>gfp</sup>/CCR2<sup>rfp</sup> (M), and CCR2<sup>rfp</sup> and Cox-2 (N). Bar represents 0.5 mm (D), 0.22 mm (H), 250  $\mu$ m (E–K) and 25  $\mu$ m (L–N). O: Quantification of CX3CR1<sup>gfp</sup>-microglia, CCR2<sup>rfp</sup>-macrophages and Cox-2-labeled cells in the peri-infarct region from NaCl- and PJ34-treated mice (n = 6 per group). Data were analyzed using a 2-way ANOVA, followed by the Newman-Keuls test. \**p* < 0.05; \*\**p* < 0.01.

### 3.3.2. Exploratory and defense behaviors

The open field test was used to assess both spontaneous exploratory and locomotor behavior and anxiety disorder, as a defense behavior. Defense behavior was also assessed by the elevated plus maze test.

The open-field test did not show any ischemia-induced disturbances for either M or F mice in exploratory behavior, as evaluated by the time spent in inactivity and the distance traveled (Fig. 6A–D). Moreover, neither ischemia nor the treatment had an effect on the number of entries into the center of the open field, which could reflect defense behavior (Fig. 6E and F). However, the time spent in the center and the distance traveled was decreased in PJ34-treated stroke M mice (Fig. 6G, *p* = 0.05 versus NaCl-treated stroke M mice), while the time spent in inactivity was not changed in F mice (Fig. 6H).

The percent time spent in the open arms of the elevated plus maze did not differ between groups for M (Fig. 7A) or F (Fig. 7B) mice. NaCl-treated M mice had an increased % number of entries in the open arms compared to PJ34-treated M mice (*p* < 0.05; Fig. 7C).

The marble-burying test is a useful test for evaluating psychiatric disorders. It has been recently proposed to evaluate impulsivity, as it evaluates anxiety-like and/or obsessive-compulsive-like behaviors (Taylor et al., 2017). The kinetics of marbles buried did not reveal any

differences between groups for M or F mice. The area under the curve, calculated from the last 20 min of the test, showed that stroke induced an increased impulsive-like behavior in M (*p* < 0.05 versus non-operated; Fig. 7G) and F (*p* < 0.05 versus non-operated; Fig. 7H) mice that was prevented by PJ34 treatment in F mice only (*p* < 0.05 versus Stroke + NaCl). No significant difference was noted between PJ34-treated M and NaCl-treated M mice (*p* = 0.124; Fig. 7G). Altogether, these results suggested that neonatal stroke could induce some modified emotional-relative behavior that could be reversed by PJ34 treatment.

### 3.3.3. Spatial learning and memory

First, during the learning phase of the Barnes Maze, all mice, M and F, exhibited similar spatial learning abilities, as the heat maps of paths taken for each group appear qualitatively similar (Supp. Fig. 7A) and as the distance traveled (Fig. 8A, B, time effect *p* < 0.0001) and the escape latency (Fig. 9A, B, time effect *p* < 0.0001) decreased during the learning phase. Likewise, learning performances for F mice did not differ between groups when comparing the calculated area under the curve (Fig. 8D). For M mice, the area under the curve for distance traveled tended to be enhanced in NaCl-treated mice (*p* = 0.052 versus non-operated; Fig. 8C).

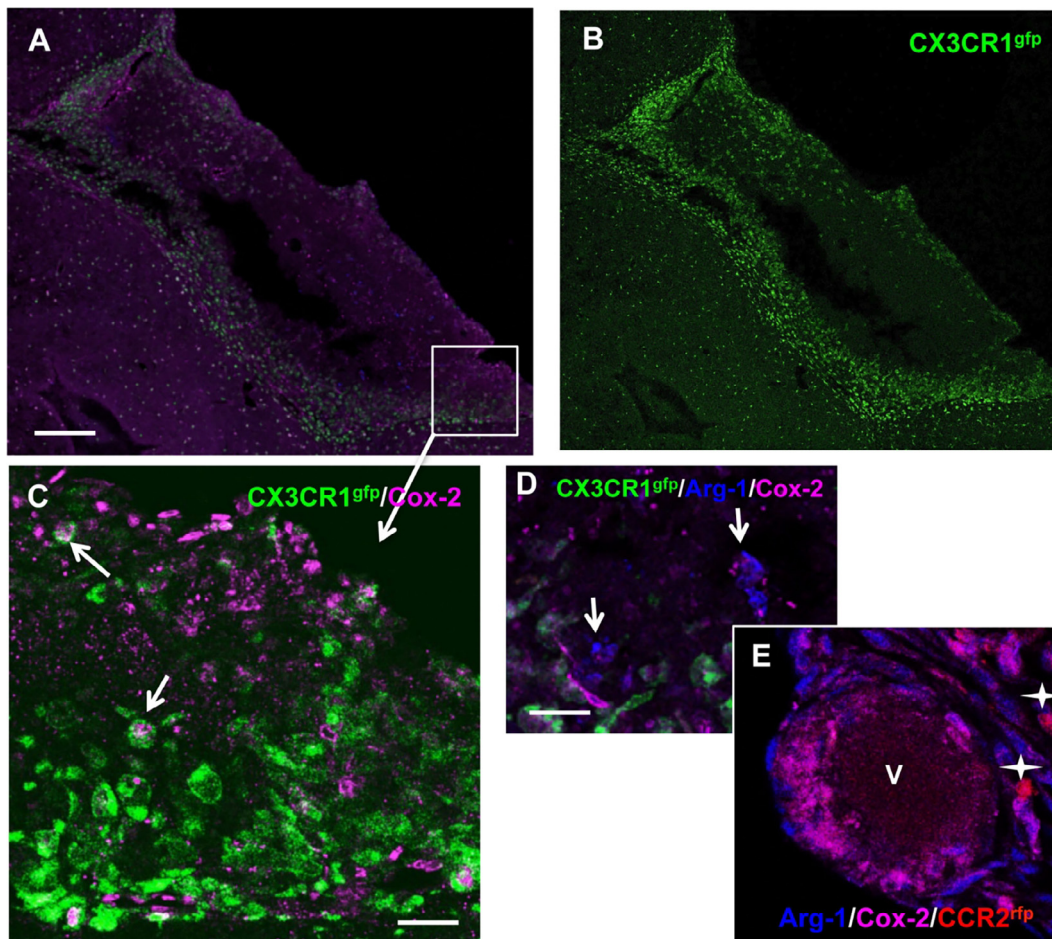


**Fig. 2.** Effect of PJ34 3 days after pMCAo on microglial activation in a 0.9% NaCl-treated CX3CR1<sup>gfp</sup>/CCR2<sup>gfp</sup> female mouse. A: Confocal merged images of labeled cells in the peri-infarct region. B: CX3CR1<sup>gfp</sup>-labeled microglia (green). C: Cox-2-positive cells (magenta) and double-labeled CX3CR1<sup>gfp</sup> and Cox-2 cells (white arrows) in the peri-infarct region. Note that Cox-2 protein often appeared as dots, suggesting a mitochondrial labeling. D-E: White arrows show Arg-1-positive cells close to the infarct region (D) and present in the vicinity of a vessel (v). In E, note the presence of 2 macrophages (CCR2<sup>gfp</sup>). Bar represents 0.4 mm (A-B) and 25  $\mu$ m (C-E).

The area under curve the calculated from the escape latency supported the tendency observed for the area under the curve for distance traveled, as it increased in NaCl-treated M mice ( $p < 0.05$  versus non-operated; Fig. 9C). These data suggested that neonatal ischemia induced a minor learning deficit that can be reversed by PJ34 in M mice only.

During the retention test, all mice showed good spatial memory performances, with no difference between groups, as the % distance traveled (see results in Supplemental Fig. 5A and B,  $p < 0.05$ ) and the % time spent were higher in the target sextant (see results in Supplemental Fig. 6A and B,  $p < 0.05$  for each group compared to the theoretical value).

Second, during the reversal learning phase, all mice also exhibited good reversal learning abilities, as the distance traveled (Fig. 8E and F, time effect  $p < 0.0001$ ) and the escape latency (Fig. 9E and F, time effect  $p < 0.0001$ ) decreased within the learning days 97 to 101. For M mice, the corresponding area under the curve did not differ between groups (Fig. 8G). Heat maps of paths taken appear qualitatively similar, as all M groups searched for the target hole in the new and the older locations (Supp. Fig. 7B). By contrast, for F mice, the area under the curve for distance traveled significantly increased in NaCl-treated stroke F mice (Fig. 8H,  $p < 0.05$  versus non-operated), demonstrating impaired learning ability, which was decreased without statistical significance by PJ34 treatment ( $p = 0.12$ ). For escape latency, for M mice, the corresponding area under the curve did not differ between groups

(Fig. 9G). For F mice, the area under the curve for escape latency increased in NaCl-treated stroke F mice (Fig. 9H,  $p = 0.086$ ), suggesting impaired learning ability, which was decreased by PJ34 treatment ( $p < 0.05$ ). Furthermore, NaCl-treated F stroke mice searched for the target hole in the new and the older location, qualitatively suggesting that stroke induces a cognitive flexibility deficit that can be abolished by PJ34 treatment (Supp. Fig. 7B).

These results showed that neonatal ischemia induced a slight deficit in spatial memory performances at 3 months, in F mice only, that was abolished by PJ34 treatment ( $p < 0.05$ ).

During the retention test at the end of the reversal learning trial, all mice showed good spatial memory performances, with no difference between groups, as the % distance traveled (see results in Supplemental Fig. 5C and D,  $p < 0.05$ ) and the % time spent were higher in the target sextant (see results in Supplemental Fig. 6C and D,  $p < 0.05$  for each group compared to the theoretical value).

### 3.3.4. Tissue loss

Three months after ischemia, tissue loss was higher in NaCl-treated M ( $17.5 \pm 4.8\%$ ,  $n = 6$ ) than in F ( $8.0 \pm 1.2\%$ ,  $n = 6$ ;  $p < 0.01$ ) mice. Two doses of PJ34 (given 1 and 3 days following ischemia) significantly reduced the hemispheric atrophy in M ( $12.0 \pm 1.5\%$ ,  $n = 6$ ;  $p < 0.01$ ), but not in F ( $7.7 \pm 2.9\%$ ,  $n = 6$ ) mice (Fig. 10A). This M-induced neuroprotective effect of PJ34 on tissue loss over the long term reflected the neuroprotective effect observed 3 days after pMCAo,

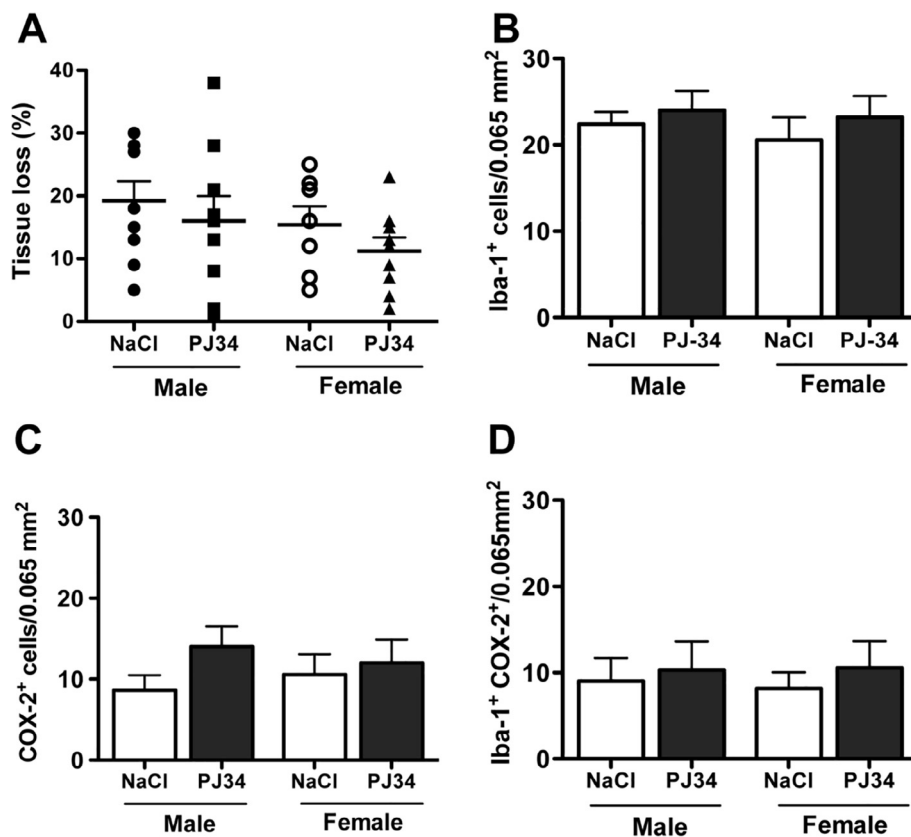


**Fig. 3.** Effect of PJ34 on tissue loss and microglial activation 8 days after pMCAo in the cortex in male (M) and female (F) C57BL/6 mice. PJ34 or NaCl was given 1 and 3 days after pMCAo. A: Tissue loss in M and F mice 8 days after pMCAo. B-D: Quantitative analysis of Iba-1<sup>+</sup> cells (B), Cox-2<sup>+</sup> cells (C), and double-labeled Iba-1<sup>+</sup>/Cox-2<sup>+</sup> cells in the peri-infarct region in both NaCl- and PJ34-treated mice. Data were analyzed using a 2-way ANOVA, followed by the Newman-Keuls test. \**p* < 0.05.

suggesting that tissue loss is an ongoing process that lasts long term after ischemia.

### 3.3.5. White matter injury

The density of MBP fibers was evaluated in the external capsule, estimated using a computerized image-analysis-based semi-quantitative method, both in the ipsilateral (IL) and contralateral (CL) hemispheres (Fig. 10B). Indeed, white matter injury (WMI) is one of the consequences of brain injury in babies that suffer from neonatal ischemic stroke. WMI is the underlying cause of motor and cognitive disability in these children. We observed that PJ34 treatment was primarily able to prevent the development of MBP fibers on the CL side, compared to the IL side in F mice.

## 4. Discussion

Only a limited number of studies have investigated the effect of sex on microglial activation after ischemic stroke in the developing brain. In this study, we examine the spatio-temporal microglial phenotype changes that occur after experimental stroke in the absence or presence of a PARP-1 inhibitor (PJ34). It was previously reported that the absence of PARP-1 preferentially protected males from perinatal injury (Hagberg et al., 2004). We report that PARP inhibition induces differential modulation of microglial phenotypes in the amygdala of male and female mice subjected to pMCAo at P9. These findings were associated with consistent differences in behavioral outcomes and myelination in adulthood.

To date, there is a lack of experimental studies evaluating adult behavioral deficits after neonatal stroke in mice. However, neonatal hypoxia-ischemia models in rats show behavioral deficits at the adult stage, such as spatial learning and memory deficits (Tsuji et al., 2010), and reference and working memory deficits (Sanchez et al., 2015; Pereira et al., 2008). In addition, motor coordination deficits (Smith et al., 2015) and novel object recognition task deficits (Pereira et al.,

2008) were studied at the juvenile age, but not in adulthood. In the present study, we provide evidence of behavioral deficits in adult mice subjected to pMCAo at P9. Neonatal ischemia induces a motor coordination deficit in both sexes, but an enhanced impulsive-like disorder and spatial learning deficits were observed only in injured female mice. These deficits are not associated with an increased mortality in female mice. These findings are relevant to the clinical observation of behavioral deficits during adulthood in patients with cerebral palsy (Frisch and Msall, 2013). Nevertheless, clinical observations and data from rodent models of neonatal ischemia report that males, in general, show an increased risk of brain-based developmental disorders (Hill and Fitch, 2012). However, in some cases, behavioral deficits after neonatal insult have been observed in females only, showing that sex affects the outcomes following neonatal stroke. To date, this effect is still poorly understood. For example, at P7 hypoxia-ischemia in rats induces juvenile cognitive deficits in both sexes, while this model, when performed at P3, induces juvenile cognitive deficits in females only (Sanchez et al., 2015). Zhu and colleagues (2006) have confirmed that sex differences could be explained by cell death pathways, involving PARP-1, in an *in vivo* model of hypoxia ischemia in mice and are likely to account for sex-specific brain damage observed in clinical and experimental studies.

Brain injury in the mature and immature brain depends on PARP-1 activation. In the early 2000s, treatment with 3-aminobenzamide (3-AB), a nonselective PARP inhibitor, reduces ischemic-reperfusion damage in both the neonatal P7 rat (Ducrocq et al., 2000) and the adult mouse by decreasing inflammation (Couturier et al., 2003). Shortly thereafter, the protective effect of PARP-1 deficiency was demonstrated to be strikingly dependent on the sex of the mice, with males being preferentially protected compared with females, in both neonatal (Hagberg et al., 2004), and adult (McCullough et al., 2005; Liu et al., 2011) brains. Rats treated with the PARP inhibitor PJ34, given after ischemia-reperfusion, showed a near-complete inhibition of microglia/macrophage activation and an 84% reduction in CA1 neuronal death

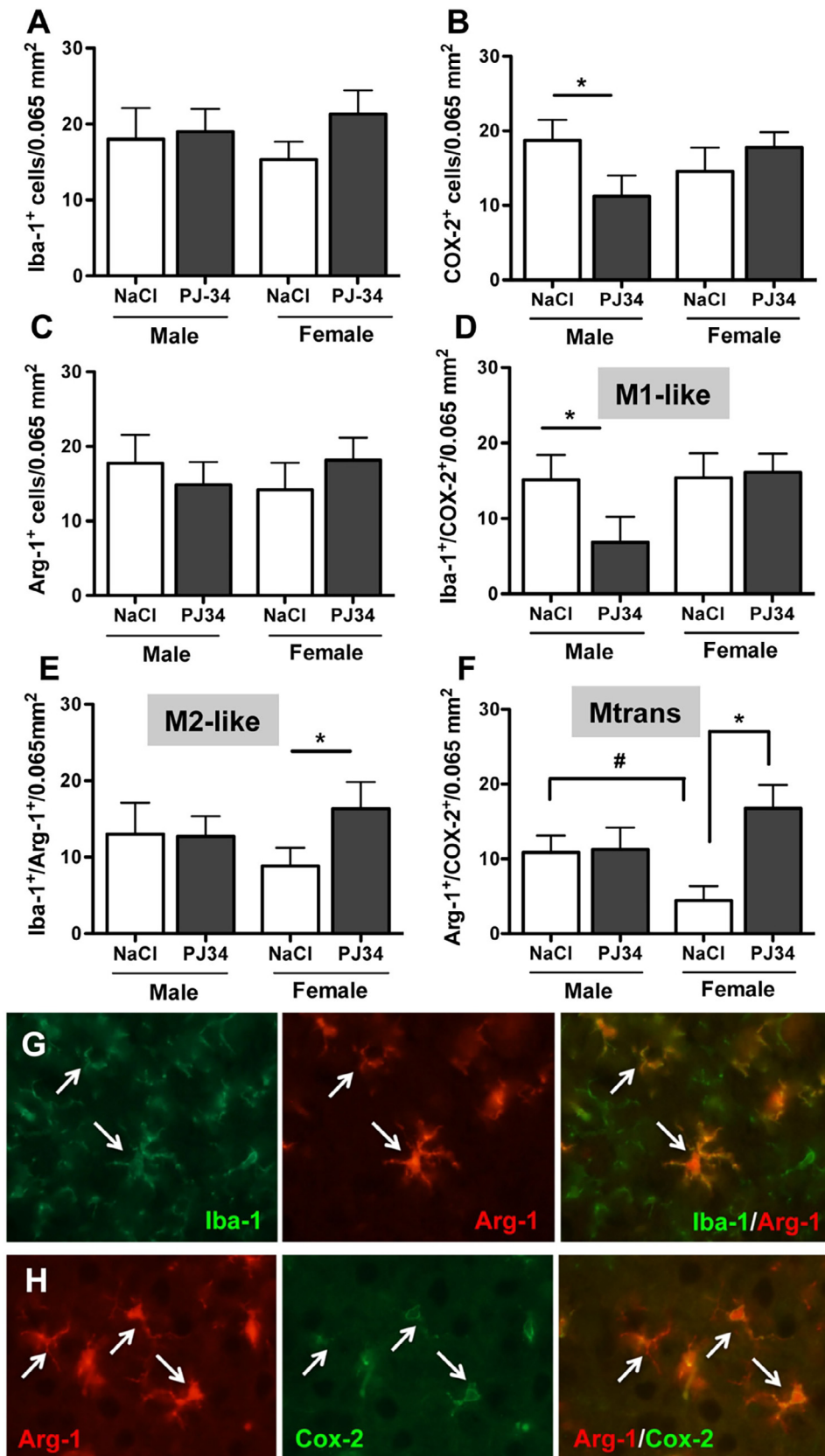


**Fig. 4.** Effect of PJ34 on microglial activation and its phenotypes 8 days after pMCAo in the amygdala of male (M) and female (F) mice. PJ34 or NaCl was given 1 and 3 days after pMCAo. A-C: Quantitative analysis of Iba-1<sup>+</sup> cells (A), Cox-2<sup>+</sup> cells (B), and Arg-1<sup>+</sup> cells (C). D-F: Quantitative analysis of double-labeled Iba-1<sup>+</sup>/Cox-2<sup>+</sup> cells (D, M1-like), double-labeled Iba-1<sup>+</sup>/Arg-1<sup>+</sup> cells (E, M2-like), and double-labeled Cox-2<sup>+</sup>/Arg-1<sup>+</sup> (F, Mtrans) cells. G-H: Typical example of double fluorescence labeling in the amygdala for Iba-1, Arg-1 and Cox-2 cells in a female mouse treated with PJ34. Data were analyzed using a 2-way ANOVA, followed by the Newman-Keuls test. \**p* < 0.05.

(Hamby et al., 2007). A delayed PJ34 treatment, from 2 up to 5 days, also enhanced long-term neuronal survival and neurogenesis (Kauppinen et al., 2009). Here, in the neonatal mouse, we found that a single injection of PJ34 preferentially reduced the ischemic lesion

3 days post-stroke in males, and, with 2 injections of PJ34, a significant reduction was observed in adult M mice. However, this sex-dependent neuroprotection was not sustained 8 days after ischemia, which could represent an intermediate time point for the establishment of

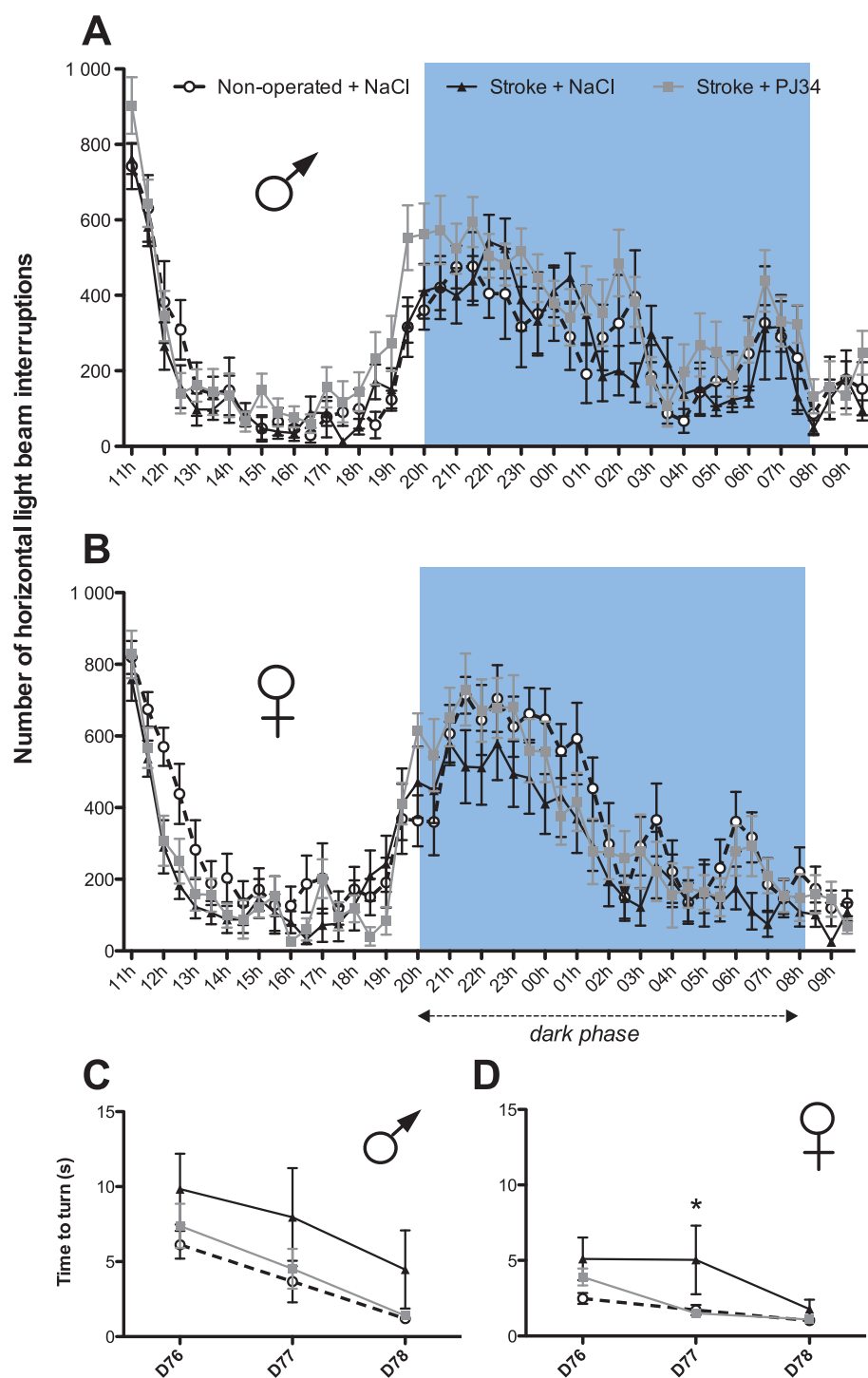


**Fig. 5.** Effect of PJ34 on spontaneous locomotor activity from days 62 to 65 after pMCAo in male (M) and female (F) mice. PJ34 or NaCl was given 1 and 3 days after pMCAo. A-B: Spontaneous locomotor activity, represented by the number of horizontal light beam interruptions for (A) M and (B) F mice. C-D: The motor coordination learning during the pole test is represented in (C) M and (D) F mice. Data collected during the actimetry test were analyzed using a 2-way ANOVA for repeated measures. Data collected during the pole test were analyzed using 2-way ANOVA for repeated measures, followed by the Dunnett test. \**p* < 0.05 versus NaCl-treated F mice.

deleterious and/or repair processes. Thus, our data highlight that the short-term outcome does not always predict the long-term outcome. In adulthood, female mice presented a decrease in tissue loss compared to male mice after neonatal stroke, suggesting that they were less sensitive to neonatal ischemia. Hypotheses might be proposed to explain this sex difference, such as epigenetics or miR (Spychala et al., 2017).

Furthermore, we reported that PJ34 treatment reduced some behavioral deficits in the adulthood in pMCAo female mice only, while brain lesions were not reduced by PJ34. Interestingly, the number, morphology and activation of microglia are different during brain development depending on the sex, suggesting that microglia might respond differently to stroke. Several studies have also demonstrated

markedly different effects of microglia for similar insults in neonatal when compared to adult brains (Mallard et al., 2018). Perinatal brain injury in CX3CR1<sup>-/-</sup> was shown to be affected by sex (Pimentel-Coelho et al., 2013). In addition, knowing the role of PARP-1 and microglia in neuroinflammation, one could suggest that PJ34-induced effects on brain lesions and associated adult behavioral disorders may originate from different microglial activation in both sexes. A reduction in the number of CX3CR1<sup>stfp</sup>-microglia was observed 3 days after stroke in PJ34-treated males compared to NaCl-treated males, strengthening the support for the anti-inflammatory properties of PJ34 and all previously reported PARP inhibitors. In the cortical peri-infarct region, an increase in CX3CR1<sup>stfp</sup>-microglia was observed 3 days after stroke in

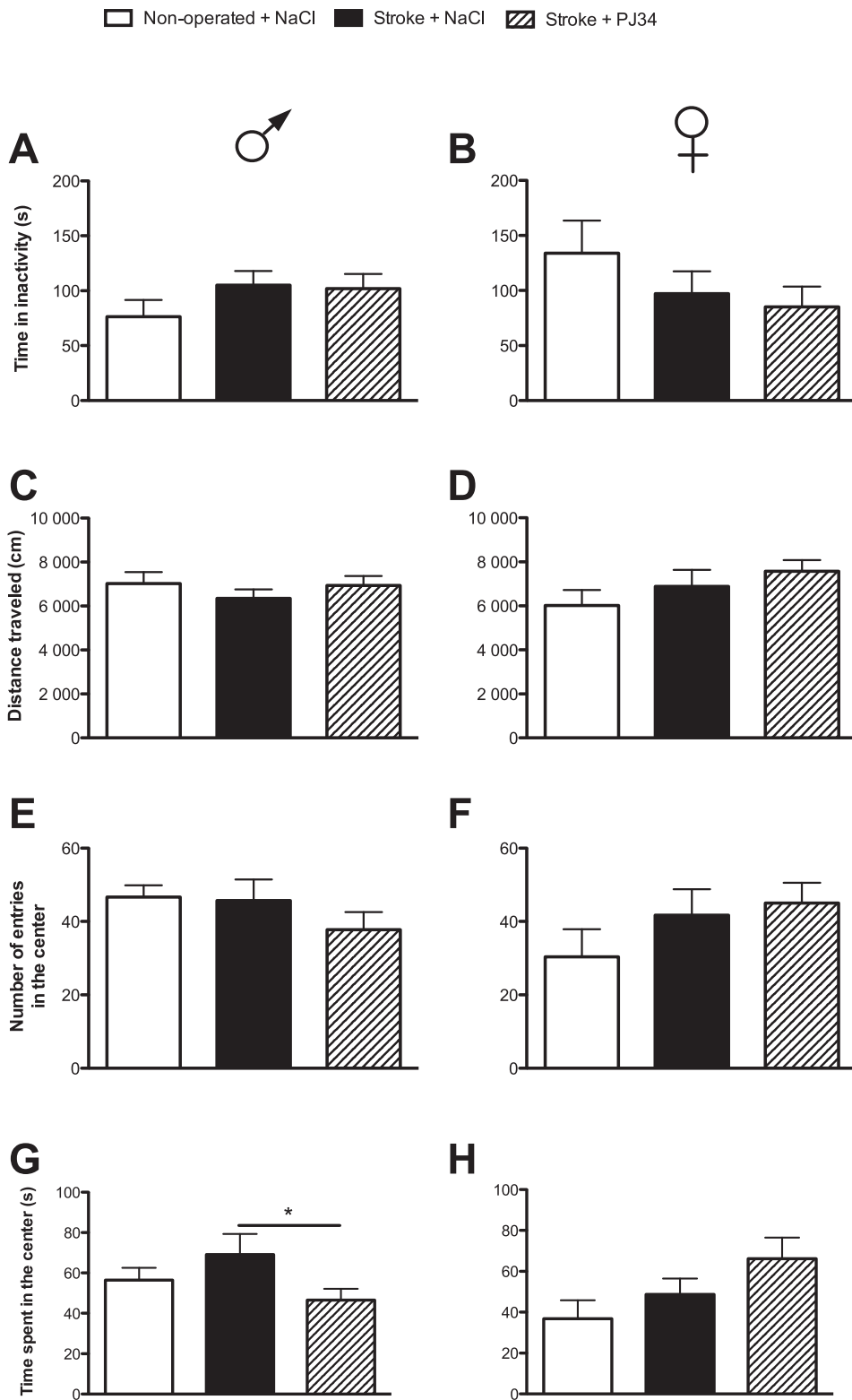


**Fig. 6.** Effect of PJ34 on locomotor activity, evaluated by data collected during the open field test from day 76 to 78 after pMCAo in male (M) and female (F) mice. PJ34 or NaCl was given 1 and 3 days after pMCAo. A-D: The time spent in inactivity and distance traveled during the open field test are represented in (A and C, respectively) for M and (B and D, respectively) for F mice. E-H: The number of entries in the center and time spent in the center during the open field test are represented in (E and G, respectively) for M and (F and H, respectively) for F mice. Data were analyzed using a one-way ANOVA, followed by the Dunnett test. \*  $p < 0.05$ .

both males and females, while CCR2<sup>flp</sup>-macrophages were sparsely observed in the lesions and peri-infarct regions. No significant differences in cell density were detected between male and females at this time-point of recovery. Microglia were the predominant myeloid cells activated after IL-1 $\beta$  challenges in the immature brain (Krishnan et al., 2017) and have pro-inflammatory and restorative functions that are essential for normal brain development (Crotti and Ransohoff, 2016; Tremblay, 2011). Adult microglia express a distinctive molecular

signature that is absent from neonatal microglia (Butovsky et al., 2014). After traumatic brain injury, male mice have a faster and more robust microglia/macrophage (Iba-1<sup>+</sup>) activation and peripheral recruitment when compared with females, leading to increased cell death and lesion volume, and this increase was measured 1, 3 and 7 days post-injury (Villapol et al., 2017). In our model, 8 days after stroke, the density of Iba-1<sup>+</sup> cells in the cortical peri-infarct region did not differ between males and females, both with and without the PJ34 treatment.

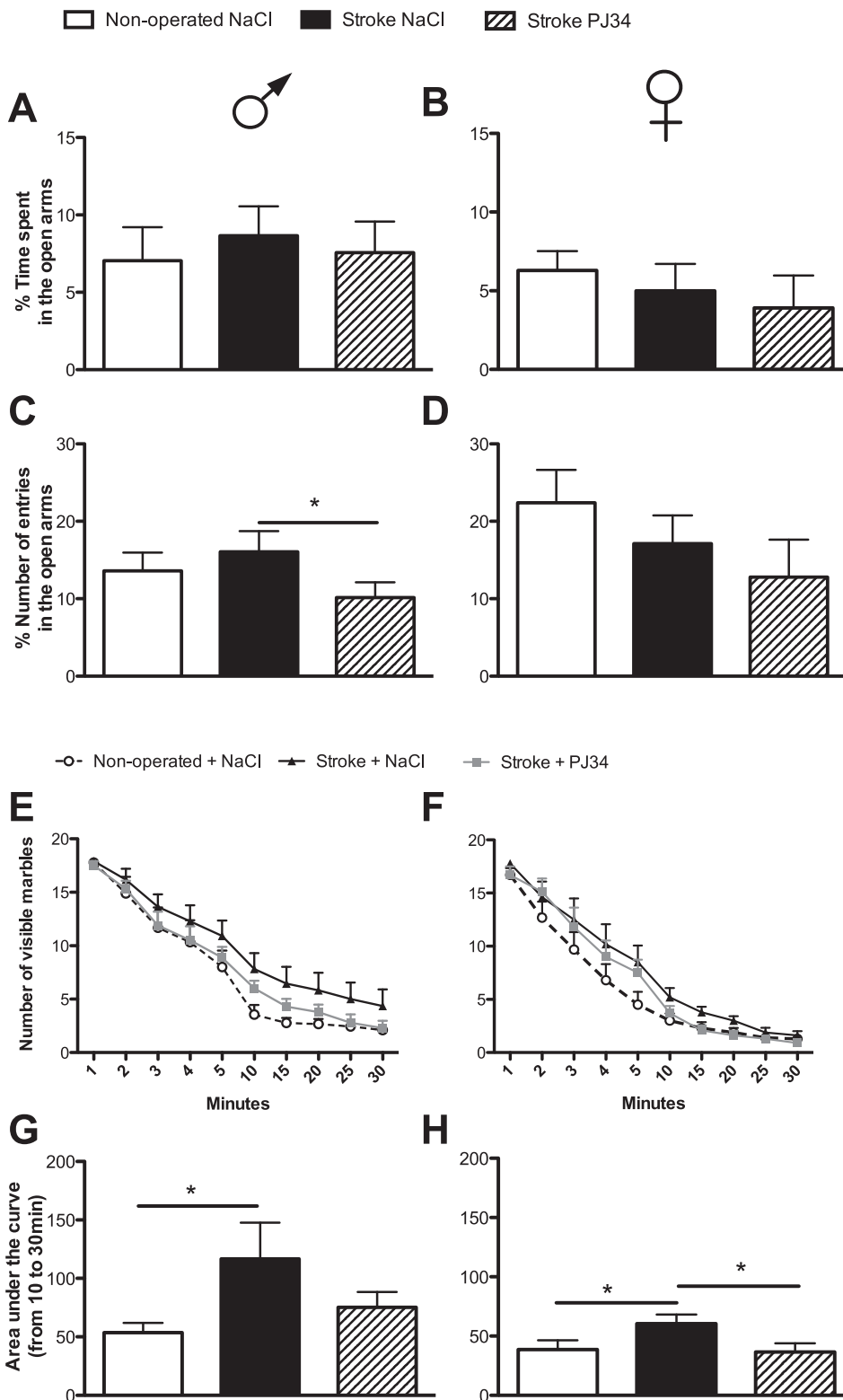
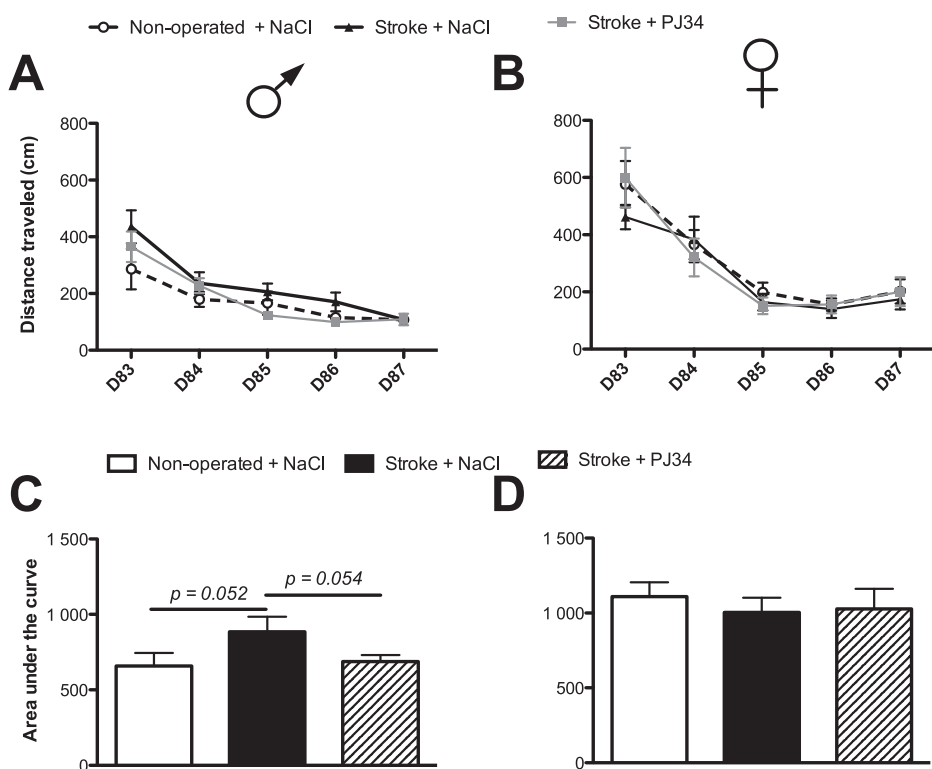


**Fig. 7.** Effect of PJ34 on defense behavior, evaluated by data collected during the elevated plus maze on days 71–72 after pMCAo, and impulsive-like behavior, evaluated by data collected during the marble-burying test on day 79 after pMCAo, in male (M) and female (F) mice. PJ34 or NaCl was given 1 and 3 days after pMCAo. A-D: The % time spent and % number of entries in the open arms are presented in (A and C, respectively) for M and (B and D, respectively) for F mice. E-H: The number of visible marbles during the 30 min test and the calculated area under curve from 10 to 30 min are presented in (E and G, respectively) for M and (F and H, respectively) for F. Data were analyzed using a one-way ANOVA, for data collected during the elevated plus maze and for the area under the curve, followed by the Dunnett test. The number of visible marbles was analyzed using a two-way ANOVA for repeated measures. \*  $p < 0.05$ .

However, in remote regions, such as the amygdala (lateral and basolateral amygdaloid nucleus), we observed degenerative neurons that could induce microglial activation. Moreover, the amygdala is a complex structure, which has a pivotal role in behavioral responses. Neonatal brain injury that primarily affects cortical neurons could modify cortico-amygdala connections, leading to the degeneration of neurons. These neurons lead to Iba-1<sup>+</sup> activated microglia with distinct

hypertrophic or bushy morphologies, expressing M1, M2 or both phenotypes (Mtrans), in both sexes. However, M2 and Mtrans phenotypes are more prevalent in injured females treated with PJ34 compared with males. Microglia are dynamic immune cells, whose numbers and morphological changes are closely associated with their functional activities. M2 polarization was suggested to be neuroprotective because sildenafil, a cyclic GMP phosphodiesterase inhibitor, increased

### Learning



### Reversal learning

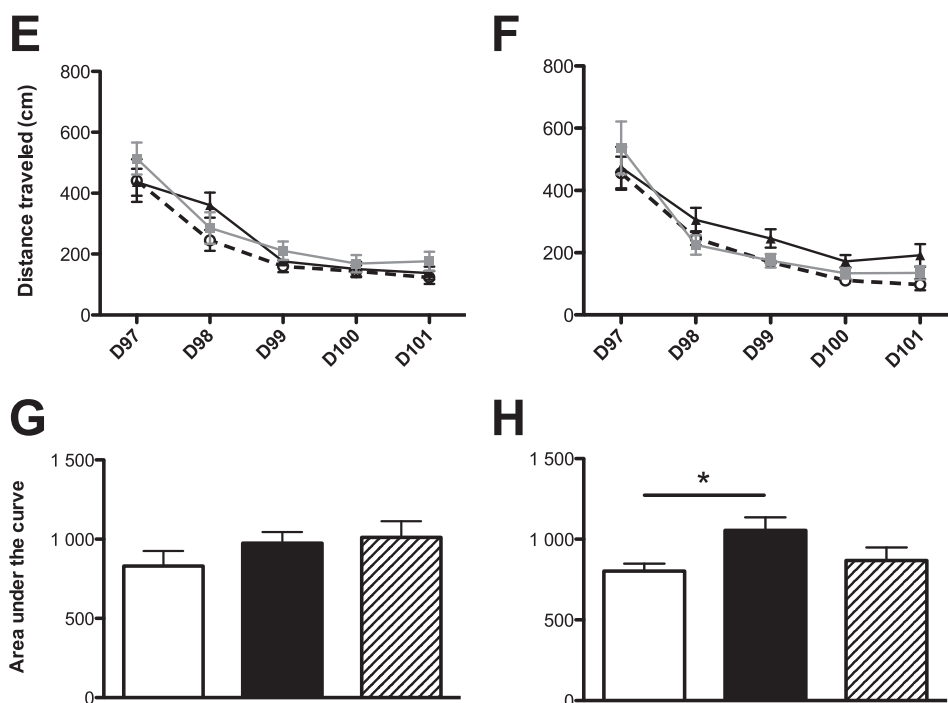
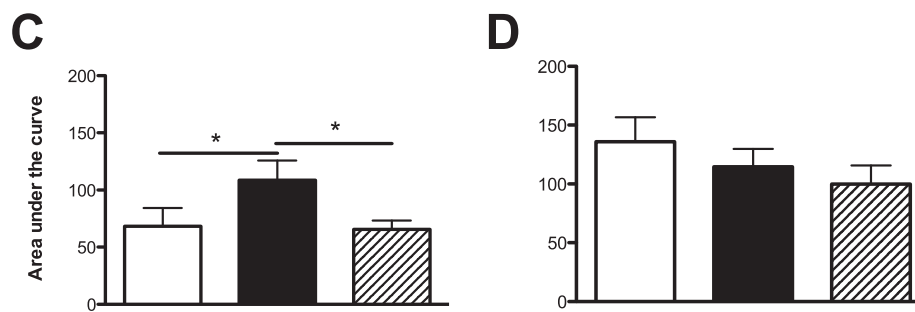
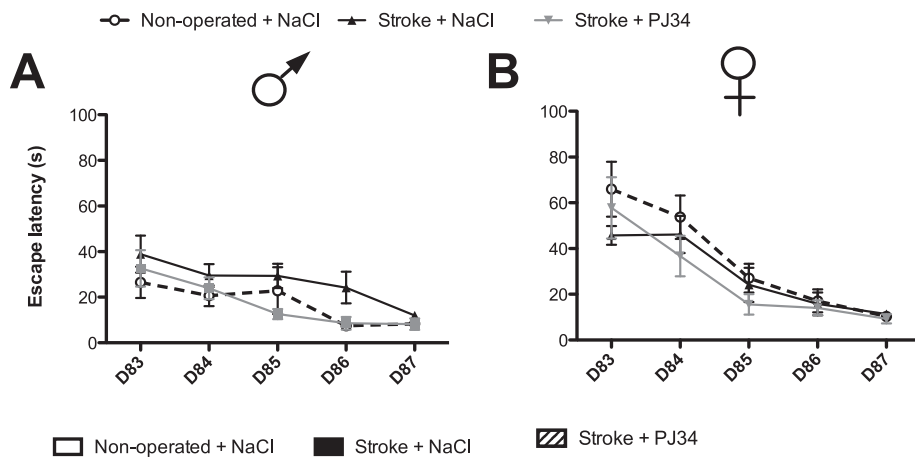


**Fig. 8.** Effect of PJ34 on spatial learning, from day 83 to 87 after pMCAo, and reversal learning, from day 97 to 101 after pMCAo, using the Barnes maze test, in male (M) and female (F) mice. PJ34 or NaCl was given 1 and 3 days after pMCAo. A-D: The distance traveled during learning is presented in (A and C) for M and (B and D) for F mice. E-G: The distance traveled during reversal learning is presented in (E and G) for M and (F and H) for F mice. Data were analyzed using a one-way ANOVA for the area under the curve analysis, and a two-way ANOVA for repeated measures for the distance traveled, followed by the Dunnett test. \**p* < 0.05.

### Learning



### Reversal learning

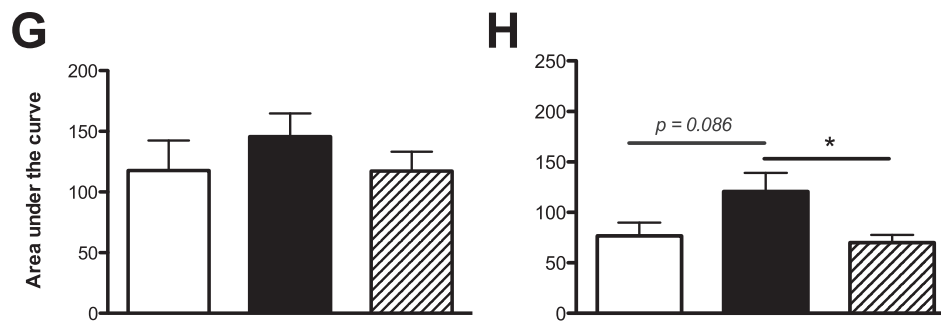
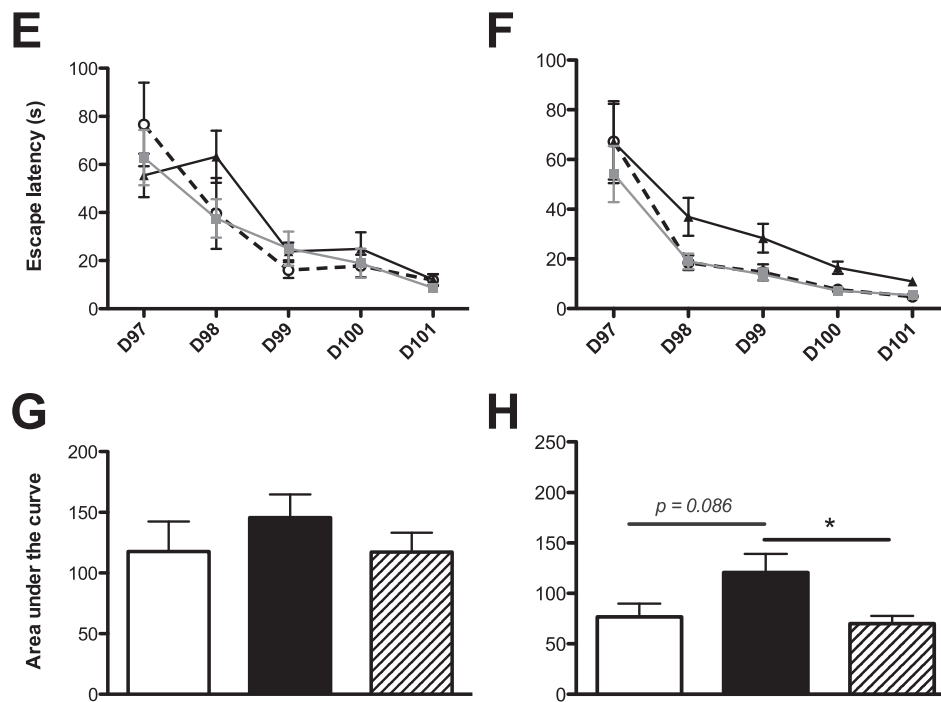


**Fig. 9.** Effect of PJ34 on spatial learning, from day 83 to 87 after pMCAo, and reversal learning, from day 97 to 101 after pMCAo, using the Barnes maze test in male (M) and female (F) mice. PJ34 or NaCl was given 1 and 3 days after pMCAo. A-D: The escape latency during learning is presented in (A and C) for M and (B and D) for F mice. E-G: The escape latency during reversal learning is presented in (E and G) for M and (F and H) for F mice. Data were analyzed using a one-way ANOVA for the area under the curve analysis, and a two-way ANOVA for repeated measures for the escape latency, followed by the Dunnett test. \* $p < 0.05$ .

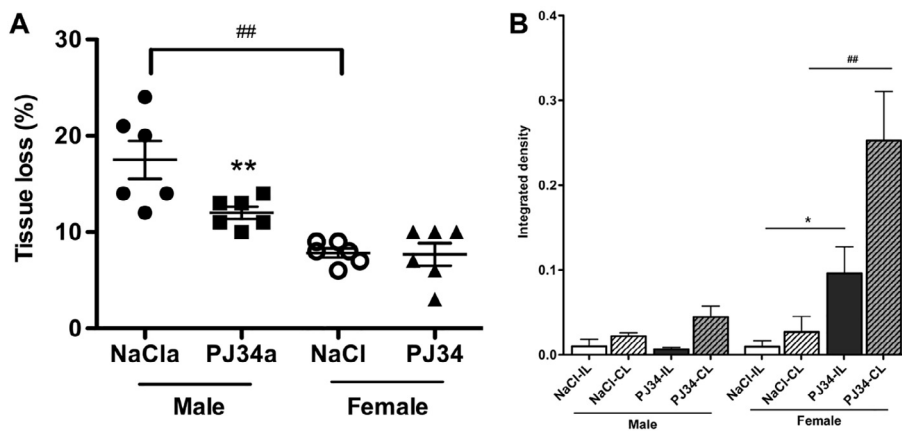


**Fig. 10.** Effect of PJ34 on tissue loss 3 months after pMCAo in CX3CR1<sup>flp</sup>/CCR2<sup>flp</sup> mice. PJ34 or NaCl was given 1 and 3 days after pMCAo. **A:** Tissue loss 3 months after pMCAo. **B:** MBP density in the external capsule 3 months after pMCAo. Data were analyzed using a one-way ANOVA, followed by the Newman-Keuls test. \* $p < 0.05$  versus NaCl-treated M mice; ## $p < 0.01$ .

polarization and reduced the lesion size after pMCAo in P9 mice (Moretti et al., 2016).

We quantified MBP density and observed that PJ34 prevents MBP fibers in F but not in M mice. These data suggest that modulating microglial activation could prevent tissue loss, preserve white matter and prevent behavioral deficits.

M2 polarization was shown to (1) promote oligodendrocyte regeneration (Miron et al., 2013) and axon regeneration in the spinal cord (Kigerl et al., 2009) and (2) be associated with improvements in long-term functional outcomes after ischemia (Suenaga et al., 2015). Our work demonstrated that the infarct volume is poorly relevant and not correlated with associated behavioral disorders in this model. However, microglial phenotypes and tissue loss over the long term could be a better predictive parameter to evaluate the effect of treatment on behavior in adulthood after neonatal stroke. In females, PJ34 increased M2 and Mtrans phenotypes in the amygdala, a brain key structure involved in attention and motivation that facilitates consolidation and memory (Tyng et al., 2017). In addition, PJ34 prevented pMCAo-induced memory disorders, such as spatial learning deficits, in adulthood, underlying the importance of the modulation of microglial phenotypes in this brain structure to improve outcomes following neonatal ischemia. The amygdala plays a central role in the social life. The amygdala shares anatomical connections with almost every other brain region that is important to social cognition, which are often collectively referred to as the “social brain”. Modifications within brain networks that modulate behavior during early development, such as after neonatal stroke, could lead to decreased connectivity between the amygdala and other brain networks.

## 5. Conclusions

Our data show that PARP inhibition differently modulates microglial phenotypes in males and females after neonatal ischemia, associated with a prevention of MBP fibers and a reduction in impulsive-like and cognitive deficits during adulthood in females only. The identification of microglial molecular pathways in both genders, and the evaluation of PARP contributions, will afford new pharmacological targets to efficiently treat males and females for neonatal stroke. Future studies on the effects of PARP inhibition on microglia transcriptomic changes and brain connectivity will greatly improve the understanding of gender-specific neuroprotection and behavioral responses of the developing brain.

## Acknowledgements

We thank Marielle Young-Ten for genotyping and the animal platform team (CRP2 – UMS 3612 CNRS – US25 INSERM-IRD, Faculté de Pharmacie de Paris, Université Paris Descartes, Paris, France) for

animal care. This work was supported by Fondation des Gueules Cassées (VCB; CML; www.gueules-cassees.asso.fr/) and Fondation pour la Recherche sur les AVC (VCB). The funders had no role in study design, data collection and analysis, decision to publish, or preparation of the manuscript.

## Appendix A. Supplementary data

Supplementary data associated with this article can be found, in the online version, at <https://doi.org/10.1016/j.bbi.2018.05.022>.

## References

- Back, S.A., 2017. White matter injury in the preterm infant: pathology and mechanisms. *Acta Neuropathol.* 134 (3), 331–349.
- Bai, P., Virág, L., 2012. Role of poly(ADP-ribose) polymerases in the regulation of inflammatory processes. *FEBS Lett.* 586 (21), 3771–3777.
- Barnes, C.A., 1979. Memory deficits associated with senescence: a neurophysiological and behavioral study in the rat. *J. Comp. Physiol. Psychol.* 93, 74–104.
- Berger, N.A., Besson, V.C., Boulares, A.H., Bürkle, A., Chiarugi, A., Clark, R.S., Curtin, N.J., Cuzzocrea, S., Dawson, T.M., Dawson, V.L., Haskó, G., Liaudet, L., Moroni, F., Pacher, P., Radermacher, P., Salzman, A.L., Snyder, S.H., Soriano, F.G., Strosznajder, R.P., Sümege, B., Swanson, R.A., Szabo, C., 2018. Opportunities for the repurposing of PARP inhibitors for the therapy of non-oncological diseases. *Br. J. Pharmacol.* 175 (2), 192–222.
- Besson, V.C., 2009. Drug targets for traumatic brain injury from poly(ADP-ribose)polymerase pathway modulation. *Br. J. Pharmacol.* 157, 695–704.
- Bouët, V., Freret, T., Toutain, J., Divoux, D., Boulouard, M., Schumann-Bard, P., 2007. Sensorimotor and cognitive deficits after transient middle cerebral artery occlusion in the mouse. *Exp. Neurol.* 203, 555–567.
- Butovsky, O., Jedrychowski, M.P., Moore, C.S., Cialic, R., Lanser, A.J., Gabrieli, G., Koegelsperger, T., Dake, B., Wu, P.M., Doykan, C.E., Fanek, Z., Liu, L., Chen, Z., Rothstein, J.D., Ransohoff, R.M., Gygi, S.P., Antel, J.P., Weiner, H.L., 2014. Identification of a unique TGF- $\beta$ -dependent molecular and functional signature in microglia. *Nat. Neurosci.* 17, 131–143.
- Charriaut-Marlangue, C., Besson, V.C., Baud, O., 2018. Sexually dimorphic outcomes after neonatal stroke and hypoxia-ischemia. *Int. J. Mol. Sci.* 19, 61.
- Chen, Y., Won, S.J., Xu, Y., Swanson, R.A., 2014. Targeting microglial activation in stroke therapy: pharmacological tools and gender effects. *Curr. Med. Chem.* 21, 2146–2155.
- Cismaru, A.L., Gui, L., Vasung, L., Lejeune, F., Barisnikov, K., Truttmann, A., Borradori Tolsa, C., Hüppi, P.S., 2016. Altered amygdala development and fear processing in prematurely born infants. *Front. Neuroanat.* 10, 55.
- Coq, J.O., Delcour, M., Massicotte, V.S., Baud, O., Barbe, M.F., 2016. Prenatal ischemia deteriorates white matter, brain organization, and function: implications for prematurity and cerebral palsy. *Dev. Med. Child Neurol.* 58, 7–11.
- Couturier, J.Y., Ding-Zhou, L., Croci, N., Plotkine, M., Margail, I., 2003. 3-Aminobenzamide reduces brain infarction and neutrophil infiltration after transient focal cerebral ischemia in mice. *Exp. Neurol.* 184, 973–980.
- Crotti, A., Ransohoff, R.M., 2016. Microglial physiology and pathophysiology: insights from genome-wide transcriptional profiling. *Immunity* 44, 505–515.
- Curtin, N.J., Szabo, C., 2013. Therapeutic applications of PARP inhibitors: anticancer therapy and beyond. *Mol. Aspects Med.* 34 (6), 1217–1256.
- Dispersyn, G., Sauvet, F., Gomez-Merino, D., Ciret, S., Drogou, C., Leger, D., Gallopin, T., Chennaoui, M., 2017. The homeostatic and circadian sleep recovery responses after total sleep deprivation in mice. *J. Sleep. Res.* 26, 531–538.
- Ducrocq, S., Benjelloun, N., Plotkine, M., Ben-Ari, Y., Charriaut-Marlangue, C., 2000. Poly(ADP-ribose) synthase inhibition reduces ischemic injury and inflammation in neonatal rat brain. *J. Neurochem.* 74, 2504–2511.
- Endres, M., Wang, Z.Q., Namura, S., Waeber, C., Moskowitz, M.A., 1997. Ischemic brain

- injury is mediated by the activation of poly(ADP-ribose)polymerase. *J. Cereb. Blood Flow Metab.* 17, 1143–1151.
- Faustino, J.V., Wang, X., Johnson, C.E., Klivanov, A., Derugin, N., Wendland, M.F., Vexler, Z.S., 2011. Microglial cells contribute to endogenous brain defenses after acute neonatal focal stroke. *J. Neurosci.* 31, 12992–13001.
- Ferrazzano, P., Chanana, V., Uluc, K., Fidan, E., Akture, E., Kintner, D.B., Cengiz, P., Sun, D., 2013. Age-dependent microglial activation in immature brains after hypoxia-ischemia. *CNS Neurol. Disord. Drug Targets* 12, 338–349.
- File, S.E., 2001. Factors controlling measures of anxiety and responses to novelty in the mouse. *Behav. Brain Res.* 125, 151–157.
- Frisch, D., Msall, M.E., 2013. Health, functioning, and participation of adolescents and adults with cerebral palsy: a review of outcomes research. *Dev. Disabil. Res. Rev.* 18, 84–94.
- Golomb, M.R., 2009. Outcomes of perinatal arterial ischemic stroke and cerebral sinovenous thrombosis. *Semin. Fetal Neonatal Med.* 14, 318–322.
- Golomb, M.R., Dick, P.T., MacGregor, D.L., Curtis, R., Sofronas, M., deVeber, G.A., 2004. Neonatal arterial ischemic stroke and cerebral sinovenous thrombosis are more commonly diagnosed in boys. *J. Child Neurol.* 19, 493–497.
- Hagberg, H., Wilson, M.A., Matsushita, H., Zhu, C., Lange, M., Gustavsson, M., Poitras, M.F., Dawson, T.M., Dawson, V.L., Northington, F., Johnston, M.V., 2004. PARP-1 gene disruption in mice preferentially protects males from perinatal brain injury. *J. Neurochem.* 90, 1068–1075.
- Hamby, A.M., Suh, S.W., Kauppinen, T.M., Swanson, R.A., 2007. Use of a poly(ADP-ribose) polymerase inhibitor to suppress inflammation and neuronal death after cerebral ischemia-reperfusion. *Stroke* 38 (Suppl 2), 632–636.
- Hill, C.A., Fitch, R.H., 2012. Sex differences in mechanisms and outcome of neonatal hypoxia-ischemia in rodent models: implications for sex-specific neuroprotection in clinical neonatal practice. *Neurol. Res. Int.* 2012, 867531.
- Hu, X., Chen, Q., Sowrirajan, B., Bosche, M., Imamichi, T., Sherman, B.T., 2017. Genome-wide analyses of microRNA profiling in interleukin-27 treated monocyte-derived human dendritic cells using deep sequencing: a pilot study. *Int. J. Mol. Sci.* 18. <http://dx.doi.org/10.3390/ijms18050925>.
- Im, H.Y., Adams Jr., R.B., Cushing, C.A., Boshyan, J., Ward, N., Kveraga, K., 2018. Sex-related differences in behavioral and amygdalar responses to compound facial threat cues. *Hum. Brain Mapp.* <http://dx.doi.org/10.1002/hbm.24035>.
- Iosif, R.E., Ekdahl, C.T., Ahlenius, H., Pronk, C.J., Bonde, S., Kokaia, Z., Jacobsen, S.E., Lindvall, O., 2006. Tumor necrosis factor receptor 1 is a negative regulator of progenitor proliferation in adult hippocampal neurogenesis. *J. Neurosci.* 26, 9703–9712.
- Jassam, Y.N., Izzy, S., Whalen, M., McGavern, D.B., El Khoury, J., 2017. Neuroimmunology of traumatic brain injury: time for a paradigm shift. *Neuron* 95, 1246–1265.
- Joly, L.M., Benjelloun, N., Plotkine, M., Charriaut-Marlangue, C., 2003. Distribution of Poly(ADP-ribosylation) and cell death after cerebral ischemia in the neonatal rat. *Pediatr. Res.* 53, 776–782.
- Kauppinen, T.M., Suh, S.W., Berman, A.E., Hamby, A.M., Swanson, R.A., 2009. Inhibition of poly(ADP-ribose) polymerase suppresses inflammation and promotes recovery after ischemic injury. *J. Cereb. Blood Flow Metab.* 29, 820–829.
- Kigerl, K.A., Gensel, J.C., Ankeny, D.P., Alexander, J.K., Donnelly, D.J., Popovich, P.G., 2009. Identification of two distinct macrophage subsets with divergent effects causing either neurotoxicity or regeneration in the injured mouse spinal cord. *J. Neurosci.* 29, 13435–13444.
- Krishnan, M.L., Van Steenwinckel, J., Schang, A.L., Yan, J., Arnadottir, J., Le Charpentier, T., Csaba, Z., Dournaud, P., Cipriani, S., Auvynet, C., Titomanlio, L., Pansiot, J., Ball, G., Boardman, J.P., Walley, A.J., Saxena, A., Mirza, G., Fleiss, B., Edwards, A.D., Petretto, E., Gressens, P., 2017. Integrative genomics of microglia implicates DLG4 (PSD95) in the white matter development of preterm infants. *Nat. Commun.* 8, 428.
- Liu, F., Lang, J., Li, J., Benashski, S.E., Siegel, M., Xu, Y., McCullough, L.D., 2011. Sex differences in the response to poly(ADP-ribose) polymerase-1 deletion and caspase inhibition after stroke. *Stroke* 42, 1090–1096.
- Mallard, C., Tremblay, M.E., Vexler, Z.S., 2018. Microglia and neonatal brain injury. *Neuroscience*. <http://dx.doi.org/10.1016/j.neuroscience.2018.03.036>.
- McCullough, L.D., Zeng, Z., Blizzard, K.K., Dechowdhury, I., Hurn, P.D., 2005. Ischemic nitric oxide and poly (ADP-ribose) polymerase-1 in cerebral ischemia: male toxicity, female protection. *J. Cereb. Blood Flow Metab.* 25, 502–512.
- Miron, V.E., Boyd, A., Zhao, J.W., Yuen, T.J., Ruckh, J.M., Shadrach, J.L., van Wijngaarden, P., Wagers, A.J., Williams, A., Franklin, R.J.M., Ffrench-Constant, C., 2013. M2 microglia and macrophages drive oligodendrocyte differentiation during CNS remyelination. *Nat. Neurosci.* 16, 1211–1218.
- Monje, M.L., Toda, H., Palmer, T.D., 2003. Inflammatory blockade restores adult hippocampal neurogenesis. *Science* 302, 1760–1765.
- Moretti, R., Leger, P.L., Besson, V.C., Csaba, Z., Pansiot, J., Di Criscio, L., Gentili, A., Titomanlio, L., Bonnin, P., Baud, O., Charriaut-Marlangue, C., 2016. Sildenafil, a cyclic GMP phosphodiesterase inhibitor, induces microglial modulation after focal ischemia in the neonatal mouse brain. *J. Neuroinflammation* 13, 95.
- Nelson, K.B., 2007. Perinatal ischemic stroke. *Stroke* 38, 742–745.
- Nissen, J.C., 2017. Microglial function across the spectrum of age and gender. *Int. J. Mol. Sci.* 18. <http://dx.doi.org/10.3390/ijms18030561>.
- Pereira, L.O., Strapasson, A.C., Nabinger, P.M., Achaval, M., Netto, C.A., 2008. Early enriched housing results in partial recovery of memory deficits in female, but not in male, rats after neonatal hypoxia-ischemia. *Brain Res.* 1218, 257–266.
- Pimentel-Coelho, P.M., Michaud, J.P., Rivest, S., 2013. Evidence for a gender-specific protective role of innate immune receptors in a model of perinatal brain injury. *J. Neurosci.* 33 (28), 11556–11572.
- Prendergast, B.J., Onishi, K.G., Zucker, I., 2014. Female mice liberated for inclusion in neuroscience and biomedical research. *Neurosci. Biobehav. Rev.* 40, 1–5.
- Ransohoff, R.M., 2016. A polarizing question: do M1 and M2 microglia exist? *Nat. Neurosci.* 19, 987–991.
- Saederup, N., Cardona, A.E., Croft, K., Mizutani, M., Coteleur, A.C., Tsou, C.L., Ransohoff, R.M., Charo, I.F., 2010. Selective chemokine receptor usage by central nervous system myeloid cells in CCR2-red fluorescent protein knock-in mice. *PLoS One* 5, e13693.
- Sanches, E.F., Arteni, N., Nicola, F., Aristimunha, D., Netto, C.A., 2015. Sexual dimorphism and brain lateralization impact behavioral and histological outcomes following hypoxia-ischemia in P3 and P7 rats. *Neuroscience* 290, 581–593.
- Schindelin, J., Arganda-Carreras, I., Frise, E., Kaynig, V., Longair, M., Pietzsch, T., Preibisch, S., Rueden, C., Saalfeld, S., Schmid, B., Tinevez, J.-Y., White, D.J., Hartenstein, V., Eliceiri, K., Tomancak, P., Cardona, A., 2012. Fiji – an open source platform for biological image analysis. *Nat. Methods* 9 (7), 676–682.
- Sharma, S., Rakoczy, S., Brown-Borg, H., 2010. Assessment of spatial memory in mice. *Life Sci.* 87, 521–536.
- Sigurdardottir, S., Indredavik, M.S., Eiriksdottir, A., Einarsdottir, K., Gudmundsson, H.S., Vik, T., 2010. Behavioural and emotional symptoms of preschool children with cerebral palsy: a population-based study. *Dev. Med. Child Neurol.* 52 (11), 1056–1061.
- Smith, A.L., Garbus, H., Rosenkrantz, T.S., Fitch, R.H., 2015. Sex differences in behavioral outcomes following temperature modulation during induced neonatal hypoxic ischemic injury in rats. *Brain Sci.* 5, 220–240.
- Spychala, M.S., Honarpisheh, P., McCullough, L.D., 2017. Sex differences in neuroinflammation and neuroprotection in ischemic stroke. *J. Neurosci. Res.* 95 (1–2), 462–471.
- Suenaga, J., Hu, X., Pu, H., Shi, Y., Hassan, S.H., Xu, M., Leak, R.K., Stetler, R.A., Gao, Y., Chen, J., 2015. White matter injury and microglia/macrophage polarization are strongly linked with age-related long-term deficits in neurological function after stroke. *Exp. Neurol.* 272, 109–119.
- Taib, T., Leconte, C., Van Steenwinckel, J., Cho, A.H., Palmier, B., Torsello, E., Lai Kuen, R., Onyeomah, S., Ecomard, K., Benedetto, C., Coqueran, B., Novak, A.C., Deou, E., Plotkine, M., Gressens, P., Marchand-Leroux, C., Besson, V.C., 2017. Neuroinflammation, myelin and behavior: temporal patterns following mild traumatic brain injury in mice. *PLoS One* 12, e0184811.
- Taylor, G.T., Lerch, S., Chourbaji, S., 2017. Marble burying as compulsive behaviors in male and female mice. *Acta Neurobiol. Exp (Wars)* 77 (3), 254–260.
- Tremblay, M.E., 2011. The role of microglia at synapses in the healthy CNS: novel insights from recent imaging studies. *Neuron Glia Biol.* 7, 67–76.
- Tsuji, M., Aoo, N., Harada, K., Sakamoto, Y., Akitake, Y., Irie, K., Mishima, K., Ikeda, T., Fujiwara, M., 2010. Sex differences in the benefits of rehabilitative training during adolescence following neonatal hypoxia-ischemia in rats. *Exp. Neurol.* 226, 285–292.
- Tyng, C.M., Amin, H.U., Saad, M.N.M., Malik, A.S., 2017. The influences of emotion on learning and memory. *Front. Psychol.* 8, 1454.
- Villapol, S., Loane, D.J., Burns, M.P., 2017. Sexual dimorphism in the inflammatory response to traumatic brain injury. *Glia* 65, 1423–1438.
- Zhu, C., Xu, F., Wang, X., Shibata, M., Uchiyama, Y., Blomgren, K., Hagberg, H., 2006. Different apoptotic mechanisms are activated in male and female brains after neonatal hypoxia-ischaemia. *J. Neurochem.* 96, 1016–1027.